The importance of intermediate range order in silicates: molecular dynamics simulation studies

Jürgen Horbach[1], Anke Winkler[1], Walter Kob[2], and Kurt Binder[1]

[1] Institut für Physik, Johannes Gutenberg–Universität, D–55099 Mainz, Staudinger Weg 7, Germany
[2] Laboratoire des Verres, Université Montpellier II, Place E. Bataillon, cc69, 34095 Montpellier, France

Abstract. We present the results of large scale computer simulations in which we investigate the structural and dynamic properties of silicate melts with the compositions $(Na_2O)2(SiO_2)$ and $(Al_2O_3)2(SiO_2)$. In order to treat such systems on a time scale of several nanoseconds and for system sizes of several thousand atoms it is necessary to use parallel supercomputers like the CRAY T3E. We show that the silicates under consideration exhibit additional intermediate range order as compared to silica (SiO_2) where the characteristic intermediate length scales stem from the tetrahedral network structure. For the sodium silicate system it is demonstrated that the latter structural features are intimately connected with a surprising dynamics in which the one–particle motion of the sodium ions appears on a much smaller time scale than the correlations between different sodium ions.

1 Introduction

Silicate melts and glasses are an important class of materials in very different fields, e.g. in geosciences (since silicates are geologically the most relevant materials) and in technology (windows, containers, optical fibers etc.). From a physical point of view it is a very challenging task to understand the properties of those materials on a microscopic level, and in the last twenty years many studies on different systems have shown that molecular dynamics computer simulations are a very appropriate tool for this purpose [1,2,3,4]. The main advantage of such simulations is that they give access to the whole microscopic information in form of the particle trajectories which of course cannot be determined in real experiments.

In *pure* silica (SiO_2) the structure is that of a disordered tetrahedral network in which SiO_4 tetrahedra are connected via the oxygens at the corners. In recent simulations we have studied in detail various aspects of static and dynamic properties of silica such as structural and thermodynamic properties of the glass state [5,6], the diffusion dynamics and structural relaxation [7,8,9,10], the frequency dependent specific heat [11], the vibrational degrees of freedom [12] and free surfaces [13,14,15]. In this paper we consider silicates that contain additional oxide components. Especially silicates

with alkali oxides have been investigated very recently in several molecular dynamics simulations [16,17,18,19,20,21,22]. We investigate here the systems $(Na_2O)2(SiO_2)$ and $(Al_2O_3)2(SiO_2)$ (for which we use in the following the abbreviations NS2 and AS2, respectively). Whereas sodium in NS2 plays the role of a network modifier that partially destroys the SiO_4 network, aluminium in AS2 is also a network former in that it prefers a four–fold coordination by oxygen atoms. However, the packing of the AlO_4 tetrahedra is different from that of the SiO_4 tetrahedra which is indicated for instance by a different coordination number distribution of aluminium and silicon by oxygen atoms (mainly two–fold for silicon and two– and three–fold for aluminium) [23]. As we show in the following the insertion of sodium or aluminium atoms does not only modify the structure on local length scales but it introduces also new intermediate length scales that can be identified by means of the partial static structure factors. These length scales are important for the dynamic properties as we will demonstrate for the case of NS2.

The rest of the paper is organized as follows: In the next section we give the main computational details and discuss the efficiency of our simulation code on the T3E at the HLRZ Stuttgart. Then we present the structural properties of AS2 and NS2 on intermediate length scales (Sec. 3) and the dynamics of NS2 (Sec. 4). Eventually we summarize our results (Sec. 5).

2 Model and details of the simulations

In a classical molecular dynamics (MD) computer simulation one solves numerically Newton's equations of motion for a many particle system. If quantum mechanical effects can be neglected such simulations are able to give in principle a realistic description of any molecular system. The determining factor of how well the properties of a real material are reproduced by a MD simulation is given by the potential with which the interaction between the atoms is described. The model potential we use to compute the interaction between the ions in NS2 and AS2 is the one proposed by Kramer *et al.* [24] which is a generalization of the so–called BKS potential [25] for pure silica. It has the following functional form:

$$\phi_{\alpha\beta}(r) = \frac{q_\alpha q_\beta e^2}{r} + A_{\alpha\beta} \exp\left(-B_{\alpha\beta} r\right) - \frac{C_{\alpha\beta}}{r^6} \quad \alpha, \beta \in [\mathrm{Si}, \mathrm{Al}, \mathrm{Na}, \mathrm{O}]. \qquad (1)$$

Here r is the distance between an ion of type α and an ion of type β. The values of the parameters $A_{\alpha\beta}, B_{\alpha\beta}$ and $C_{\alpha\beta}$ can be found in the original publication. The potential (1) has been optimized by Kramer *et al.* for zeolites, i.e. for systems that consist of Si, Al, Na, O, and possible other components like phosphor. In that paper the authors used for silicon, aluminium, and oxygen the *partial* charges $q_{\mathrm{Si}} = 2.4$, $q_{\mathrm{Al}} = 1.9$, and $q_{\mathrm{O}} = -1.2$, respectively, whereas sodium was assigned its real ion charge $q_{\mathrm{Na}} = 1.0$. Thus, with this set of charges charge neutrality is fulfilled neither in NS2 nor in AS2. We

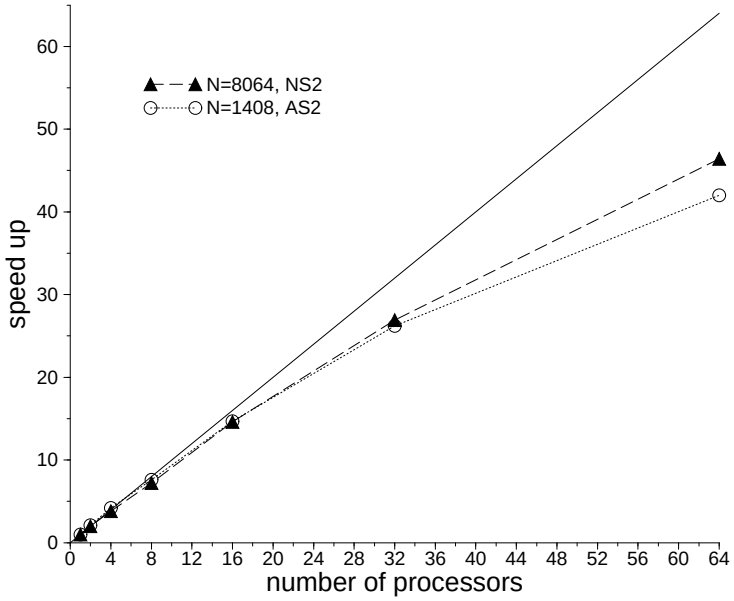

Fig. 1. Speed up factor for the simulations with $N = 8064$ (filled triangles) and $N = 1408$ particles (open circles) as a function of the number of processors n. The bisecting line (straight line) indicates a perfect scaling of the performance with n.

have therefore modified the Kramer potential by setting the partial charge for sodium and aluminium to 0.6 and 1.8, respectively, and by introducing additional short range potentials such that the original functional form of the Kramer potential is approximately recovered on distances of nearest Al–O and Na–O neighbors. More details on the interaction potential can be found in Refs. [16,17,23]. Our models give predictions for structural and dynamic properties of NS2 and AS2 which are in good agreement with experimental findings [17,23]. Furthermore, Ispas *et al.* [26] have shown for $(Na_2O)4(SiO_2)$ that *ab initio* simulations (Car–Parrinello molecular dynamics) yield comparable results regarding the structure to those obtained with molecular dynamics simulations in which our potential model is used.

The simulations have been done at constant volume: For AS2 we fixed the density to $2.6\,\mathrm{g/cm^3}$ which is close to the experimental density at $T = 300$ K. In the case of NS2 we did simulations at the two densities $2.37\,\mathrm{g/cm^3}$ and $2.5\,\mathrm{g/cm^3}$, corresponding to experimental densities in the melt and at room temperatures, respectively. The AS2 system consists of 1480 particles and for the NS2 systems we used system sizes of 8064 particles at the low density and 1152 particles at the high density.

As can be seen from Eq. 1 the interaction potential contains a long–ranged Coulomb term. This part of the interaction is the most time consuming in the calculation of the forces. To do this we made use of the so–called Ewald summation technique [27], a method that scales with the particle number N as $N^{3/2}$. Thus, for systems which contain about 8000 particles a huge numerical effort is required: The longest runs (at the lowest temperatures) had a length of about 10 million time steps for which a time of two weeks was needed on 64 processors thus giving a total CPU time of about 128 weeks of (single) processor time.

The equations of motion were integrated with the velocity form of the Verlet algorithm. The time step of the integration was 1.6 fs. The temperature range investigated was 4000 K$\geq T \geq$ 2100 K in the case of NS2 and 6100 K$\geq T \geq$ 2300 K in the case of AS2. To equilibrate the systems the temperatures were controlled by coupling them to a stochastic heat bath, i.e. by substituting periodically the velocities of the particles with the ones from a Maxwell-Boltzmann distribution with the correct temperature. After the system was equilibrated at the target temperature, we continued the run in the microcanonical ensemble, i.e. the heat bath was switched off. We have done production runs up to several ns real time which corresponds to several million time steps. We have also calculated glass structures at $T = 300$ K. The glass state was produced by cooling the system from equilibrated configurations at our lowest temperatures with a cooling rate of about 10^{12} K/s. Note that we show in the following sections only results for the lowest temperatures, i.e. at $T = 2100$ K for NS2 and at $T = 2300$ K for AS2 as well as at $T = 300$ K for both systems, because the results for the higher temperatures lead essentially to the same conclusions that we will draw below. However, a detailed discussion of the temperature dependence of the systems under consideration can be found in Refs. [17].

The program code was written in FORTRAN. All the parallelization was done by using MPI subroutines. More details on the parallelization can be found in Refs. [9,23]. Of course, the performance of a parallel code never scales perfectly with the number of processors because the communication between the processors requires an additional amount of CPU time. Fig. 1 shows the speed up factor on the Cray T3E of the HLRZ Stuttgart as a function of the number of processors n, i.e., the factor by which the code is faster if one uses n processors instead of one. The bisecting line indicates the limiting case where the communication overhead is not influenced by the speed of the code. We see that the curves for $N = 1408$ and $N = 8064$ scale nearly perfectly for $n \leq 16$. For $n = 64$ we obtain still a speed up factor of about 46.4 for $N = 8064$ particles whereas this factor is 42 for $N = 1408$. In most of our simulations we have used 64 processors for the large systems and 32 processors for the small ones.

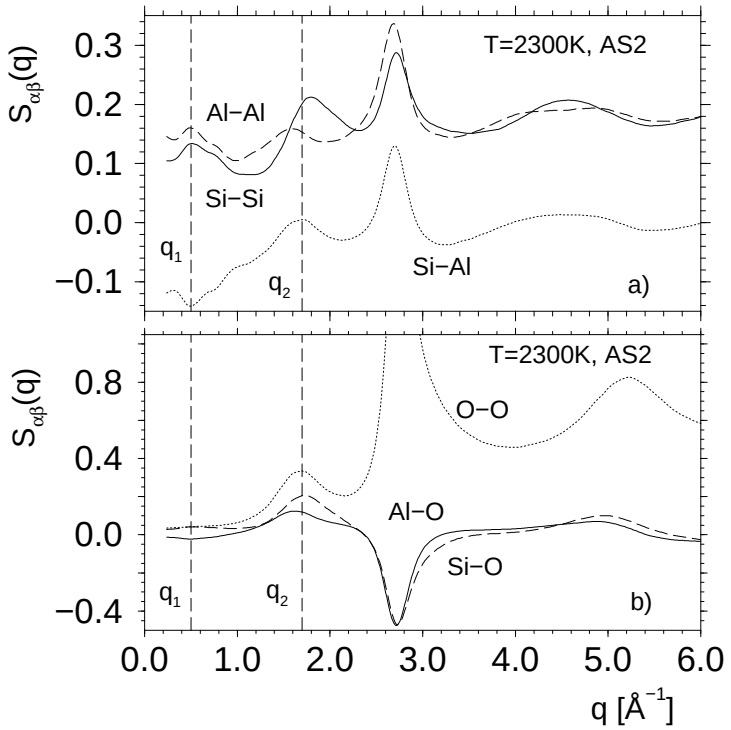

Fig. 2. Partial static structure factors for AS2 at $T = 2300$ K. a) Al–Al, Si–Si, and Si–Al correlations, b) Si–O, Al–O, and O–O correlations. For the meaning of the dashed vertical lines see text.

3 Intermediate length scales in silicates

An appropriate quantity to investigate the structure of atomic systems on intermediate length scales is the static structure factor. It is essentially the Fourier transform of the pair correlation function which gives the probability of finding an atom at a distance r from another atom [2]. The structure factor can be directly measured in neutron scattering experiments from the intensity of the radiation observed with a momentum transfer $\hbar\mathbf{q}$ ($\hbar$: Planck's constant, $\mathbf{q}$: wave–vector of the momentum transfer). In a three–component system one can define six partial structure factors as [2]

$$S^{\alpha\beta}(q) = \frac{1}{N} \sum_{k=1}^{N_\alpha} \sum_{l=1}^{N_\beta} \langle \exp\left(i\mathbf{q} \cdot [\mathbf{r}_k - \mathbf{r}_l]\right) \rangle \,. \tag{2}$$

where the first sum runs over N_α particles of type α and the second one over N_β particles of type β.

Fig. 2 shows $S_{\alpha\beta}(q)$ for AS2 at the temperature $T = 2300$ K. For $q > 2.3$ Å^{-1} the partial structure factors reflect length scales of nearest neigh-

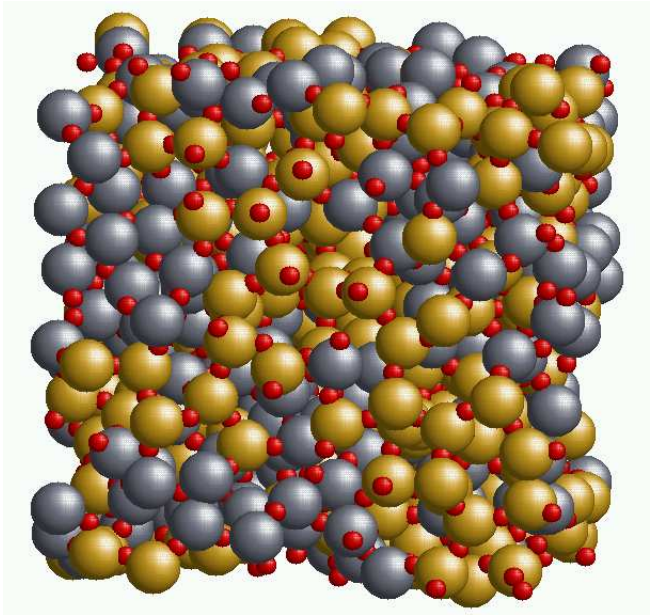

Fig. 3. Snapshot of $(Al_2O_3)2(SiO_2)$ (AS2) at $T = 300$ K. The size of the spheres is chosen such that one can identify aluminium– and silicon–rich regions: The aluminium and oxygen atoms are shown respectively as big blue and gold spheres, whereas the oxygen atoms are shown as small red spheres.

bors. In AS2 the smallest distances between atoms are those of Al–O and Si–O bonds that have lengths of about 1.6 to 1.65 Å. The peaks around $q_2 = 1.7$ Å^{-1} in $S_{\alpha\beta}(q)$ (marked by dashed vertical lines in Fig. 2) are due to the order that arises from the tetrahedral network structure. The length scale $2\pi/1.7$ Å^{-1} $= 3.7$ Å that corresponds to this peak is approximately the spatial extent of connected SiO_4 and AlO_4 tetrahedra. Note that in silica a peak at 1.7 Å^{-1} is also a very prominent feature and is called there first sharp diffraction peak. But in contrast to silica one observes in AS2 an additional peak at $q_1 = 0.5$ Å^{-1} in the Al–Al, Si–Si, and Si–Al correlations and only weakly pronounced also in the remaining correlations in which oxygen is involved. q_1 corresponds to a length scale of about 12.5 Å and has its reason in a slightly different ordering of AlO_4 complexes as compared to the SiO_4 network (for details see [23]). This relatively large length scale shows that large system sizes are required to analyze the structure of systems like AS2 in a sensible way. The different ordering of AlO_4 leads to a structure where an AlO_4 tetrahedron prefers to be surrounded on a local scale by other AlO_4 tetrahedra. This leads to a structure where AlO_4 complexes are connected to each other as string–like objects through the system that form a percolating network. This is illustrated by the snapshhot in Fig. 3 where the aluminium and silicon atoms are shown as the blue and gold spheres, respec-

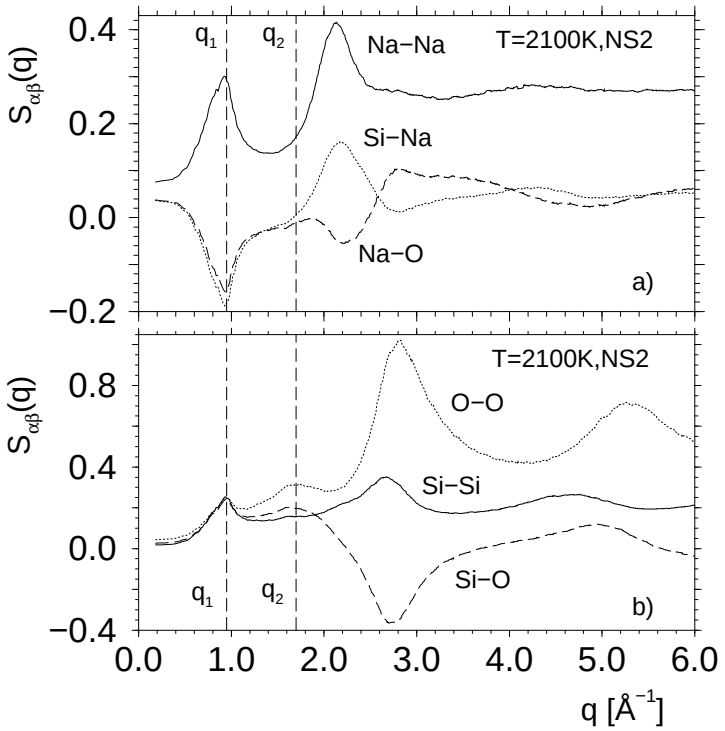

Fig. 4. Partial static structure factors for NS2 at $T = 2100$ K. a) Na–Na, Si–Na, and Na–O correlations, b) Si–O, Si–Si, and O–O correlations. For the meaning of the dashed vertical lines see text.

tively. Note that it does not matter that this snapshot is at $T = 300$ K and not at $T = 2300$ K as the structure factors in Fig. 2 because we find only small differences in structural quantities at both temperatures. Thus, we see that the aluminium atoms are not at all homogeneously distributed and if one only considers the Al atoms voids with a size of about $2\pi/q_1$ are found that lead to the peak at q_1 in $S_{\mathrm{Al-Al}}$. It is not surprising that these voids are also reflected in the Si–Si and Si–Al correlations but much less in the correlations containing oxygen (as can be seen in Fig. 2b): The oxygen atoms are essentially homogeneously distributed on the length scale $2\pi/q_1$ since they are nearest neighbors of silicon and aluminium with a similar length of Si–O and Al–O bonds.

The sodium ions in NS2 play a different role from the aluminium atoms in AS2 since they partially destroy the SiO_4 network. This can be directly recognized in the partial structure factors for NS2 which are shown in Fig. 4 at $T = 2100$ K for the density $\rho = 2.37$ g/cm^3: The peak at $q_2 = 1.7$ Å^{-1} that reflects the structure of a tetrahedral network is absent in the correlations with sodium (Fig. 4a) and is especially in $S_{\mathrm{Si-Si}}$ much weaker pronounced

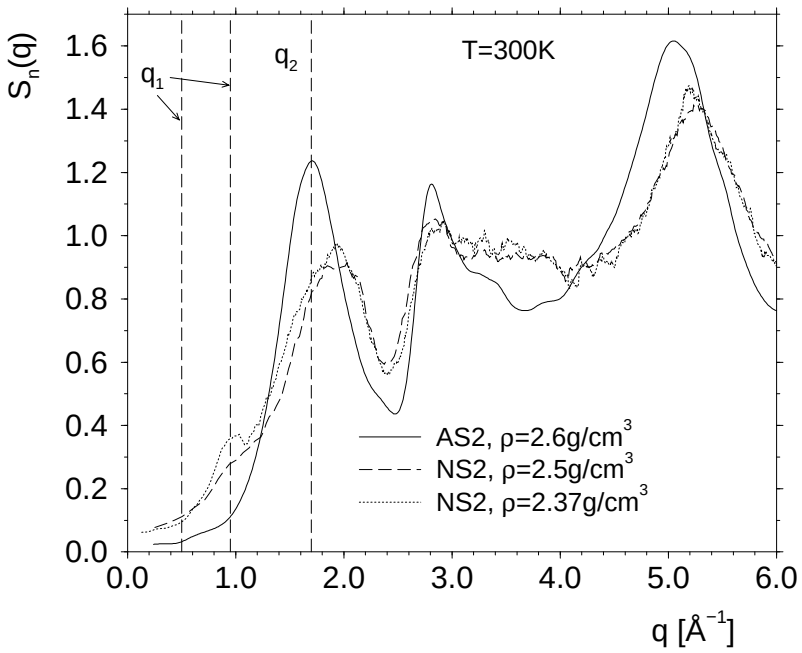

Fig. 5. $S_{\rm n}(q)$ at $T = 300$ K for AS2 and for NS2 at the indicated densities. The dashed vertical lines mark the position of the peaks at $q_1 = 0.5$ Å^{-1} in AS2, $q_1 = 0.95$ Å^{-1} in NS2, and $q_2 = 1.7$ Å^{-1} in both systems.

than in AS2 (Fig. 4b). But we observe again a second prepeak at smaller q, now around $q_1 = 0.95$ Å^{-1}. This q value is of the order of the length scale of next nearest Na–Na or Si–Na neighbors (around 6.6 Å). Again, the peak at q_1 is the characteristic wave–vector of a percolating network that is now formed by the sodium atoms. At first glance it seems to be surprising that also $S_{\rm O-O}$ exhibits a peak at q_1. But the role of oxygens is different in NS2 from that in AS2: The nearest neighbor distance for Na–O, 2.2 Å, is larger than for Si–O which is 1.6 Å. And the arrangement of oxygen around sodium is different from the tetrahedral one around silicon (for more details see Ref. [17]). Thus, the distribution of oxygen atoms in NS2 is not homogeneous on the length scale $2\pi/q_1$.

So far we have seen that NS2 and AS2 exhibit intermediate order on a relatively large length scales. This gives rise to a prepeak in $S_{\alpha\beta}(q)$ at q_1 which is 0.5 Å^{-1} for AS2 and 0.95 Å^{-1} for NS2. But does one see these peaks at q_1 also in experiments? In experiments such as neutron scattering one does not have access to the partial structure factors for systems like NS2 or AS2. Here one measures a sum of the partial structure factors whereby the

different contributions are weighted by the neutron scattering lengths b_α:

$$S_{\rm n}(q) = \frac{1}{\sum_\alpha N_\alpha b_\alpha^2} \sum_{kl} b_k b_l \left\langle \exp\left(i\mathbf{q}\cdot[\mathbf{r}_k - \mathbf{r}_l]\right)\right\rangle . \tag{3}$$

The values for b_α are $0.4149{\cdot}10^{-12}$ cm, $0.3449{\cdot}10^{-12}$ cm, $0.363{\cdot}10^{-12}$ cm, and $0.5803{\cdot}10^{-12}$ cm for silicon, aluminium, sodium, and oxygen, respectively [28]. By weighting the $S_{\alpha\beta}(q)$ from our simulation with the b_α in accordance with Eq. (3) one can easily calculate the quantity $S_{\rm n}(q)$. It is shown in Fig. 5 at $T = 300$ K for NS2 at the two densities $\rho = 2.37$ g/cm^3 and 2.5 g/cm^3 and for AS2 at $\rho = 2.6$ g/cm^3. We infer from this figure that the aforementioned prepeaks at q_1 can be seen in AS2 and in NS2 at the higher density only as a weakly pronounced shoulder. Thus it would be difficult to identify them in a neutron scattering experiment. Only in NS2 at the lower density one can clearly see the prepeak at $q = 0.95$ Å^{-1}. But at this density we observe a negative pressure of about -1.6 GPa at $T = 300$ K, a condition that would be difficult to realise in an experiment. However, in an experiment under normal pressure conditions the density decreases if one goes to higher temperatures. And indeed, very recent neutron scattering experiments of Meyer *et al.* do find the feature at q_1 for NS2 [29]. Meyer *et al.* have measured for the first time the temperature dependence of the structure factor from $T = 300$ K (where the system is in a glass state) to $T = 1600$ K (where one has a melt). They find that the feature at q_1 becomes more and more pronounced by increasing the temperature and one can clearly identify it at $T = 1600$ K. This behavior is similar to what we see in our simulations and can be understood by an decreasing density in the experiment if the temperature is increased.

4 The dynamics of NS2

In a recent simulation we have demonstrated that the dynamics in in NS2 is much faster than the one in pure silica [17]. Even at a relatively high temperature of $T = 2750$ K the diffusion constants of silicon and oxygen are two orders of magnitude larger in NS2 than in SiO_2. Furthermore, in NS2 the sodium diffusion decouples more and more from the silicon and oxygen diffusion such that at temperatures $T \leq 2500$ K the dynamics of the Na atoms is about two orders of magnitude faster than the one of the oxygen and silicon atoms [17]. This is in qualitative agreement with the expermental fact that NS2 is an ion conducting material.

Thus, since essentially the Si and O atoms do not move with respect to the movement of the Na atoms one may expect that sodium diffusion is restricted to a small subspace of the configuration space. The Si and O atoms form a quasi–frozen matrix for the Na atoms and it would be surprizing if the sodium atoms are able to diffuse into this matrix. In order to check this idea we have calculated a (coarse grained) probability of finding *no* sodium atom at a given location in space. Following the approach of Jund *et al.* [19]

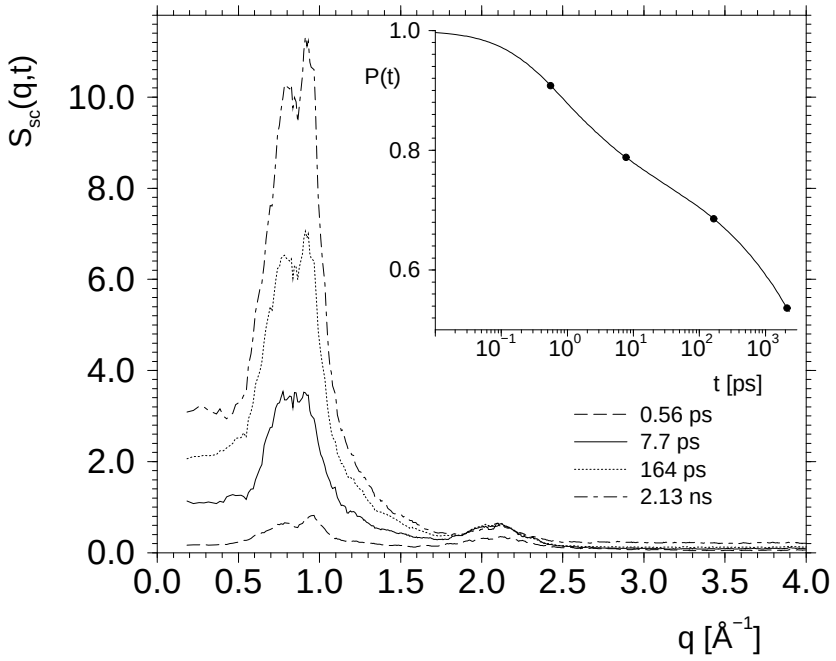

Fig. 6. Swiss cheese structure factor $S_{\rm sc}(q,t)$ at the indicated times. The inset shows the probability $P(t)$ (see text). The circles on the curve for $P(t)$ are at the times at which $S_{\rm sc}(q,t)$ is shown.

we calculate this probability by dividing the system into 48^3 cubes (of length $L/48 \approx 1.01$ Å). Then we calculate the probability $P(t)$ that a cube which does not contain a sodium ion at time zero is also not visited by a sodium ion until a later time t. The time dependence of $P(t)$ is shown in the inset of Fig. 6. From this graph we recognize that after 2.5 ns, i.e. after more than the $\alpha-$relaxation time of the matrix [17], more than 50% of the cubes have not yet been visited by a sodium atom. (We mention that after this time the mean squared displacement of the Na atoms is more than $(45$ Å$)^2$, which shows that these atoms have moved a large distance. On this time scale also the *local* structure of the Si–O matrix is partially reconstructed [17].) Hence we can conclude that on this time scale the sodium free region forms a percolating structure around a network of channels, i.e. it has somewhat the structure of a Swiss cheese. In order to investigate the structure of this percolating region we define a "Swiss cheese" structure factor $S_{\rm sc}(q,t)$ as follows: We assign to each cube which has not been visited by a sodium atom until time t a point and we compute the static structure factor of $N_{\rm sc}(t) = P(t)(48^3 - N_{\rm Na})$

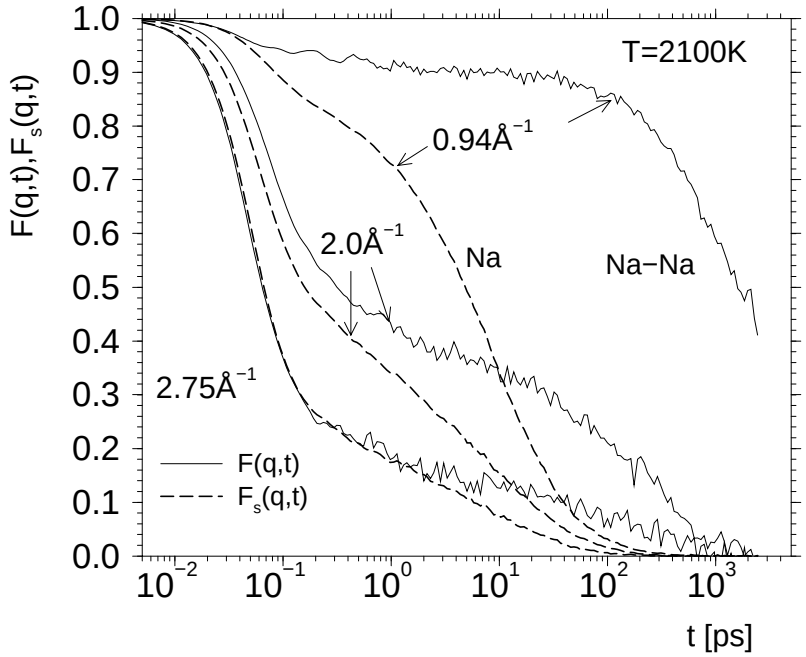

Fig. 7. Coherent intermediate scattering functions $F(q,t)$ for sodium–sodium correlations (bold solid lines) and incoherent intermediate scattering functions $F_{\rm s}(q,t)$ (dashed lines) at $T = 2100$ K for the indicated values of q.

points:

$$S_{\rm sc}(q,t) = \frac{1}{N_{\rm sc}(t)} \sum_{k,l=1}^{N_{\rm sc}(t)} \langle \exp(i\boldsymbol{q}\cdot(\boldsymbol{r}_k - \boldsymbol{r}_l))\rangle \ . \tag{4}$$

This quantity is shown in Fig. 6 for four different times: $t = 0.56$ ps, 7.7 ps, 164 ps, and 2.13 ns. We see that $S_{\rm sc}(q,t)$ has a pronounced peak at $q_1 = 0.95$ Å^{-1} which is also a prominent feature in $S_{\rm Na-Na}(q)$, as we have seen in the preceding section. Hence we can now conclude that the peak at q_1 in $S_{\rm Na-Na}(q)$ corresponds to the typical distance between the channels. Note that with increasing time the height of this peak increases quickly. However, it is clear that the peak at q_1 decreases again on the time scale on which the matrix starts to reconstruct itself significantly and thus rearranges the channel structure.

We address now the question how the sodium ions relax inside the channels. An appropriate quantity to investigate this point are time dependent density–density correlation functions, i.e. the coherent intermediate scattering function $F(q,t)$ and its self part, the incoherent intermediate scattering

function $F_s(q,t)$ [2]. In Fig. 7 we show $F(q,t)$ for the Na–Na correlations (solid lines) as well as $F_s(q,t)$ for the sodium atoms (dashed lines) for three different wave–vectors: $q = 0.94$ Å^{-1}, 2.0 Å^{-1}, and 2.75 Å^{-1}. From this figure we infer immediately a surprising result: At $q = 0.94$ Å^{-1}, i.e. at the characteristic q value of the sodium channel structure, $F(q,t)$ decays on a time scale which is two orders of magnitude larger than the one for $F_s(q,t)$. Such a strong difference cannot be explained by a de Gennes narrowing argument [2]. Instead this result can be rationalized by the idea that the sodium atoms move quickly between preferential sites, since this type of motion gives rise to a fast decorrelation of the incoherent function whereas it does not affect the coherent one. Only on the time scale of the relaxation of the SiO_2 matrix also the coherent function starts to decay. Note that the slow decay of $F(q,t)$ is found only for wave–vectors around 0.95 Å^{-1}. For different q the function decays significantly faster as can be seen from the other curves shown in Fig. 7.

More details on the issues discussed in this section can be found in Ref. [18].

5 Summary

Large scale molecular dynamics computer simulations as the ones presented in this paper for AS2 and NS2 require the use of parallel computers such as the Cray T3E. Only then it is possible to simulate these systems on a scale of several ns for system sizes which are big enough to study the structure and dynamics on intermediate length scales (up to 8000 particles in our case). Although no neutron scattering experiments can be done yet for temperatures above 2000 K, the structural and dynamical properties are already present at these high temperatures and thus, one can gain insight into features that one observes in experiments. Furthermore, this insight is much more detailed in a MD simulation than in an experiment since one has access to the full microscopic information in form of the particle trajectories.

We have exploited this fact for the case of AS2 and NS2 by showing that these systems exhibit intermediate range order on length scales that are larger than the one given from the tetrahedral network structure in *pure* silica. The reason for this is a different ordering of Al–O and Na–O complexes and leads to a percolating network of these structural elements through the SiO_4 network. We have shown for the example of NS2 that this intermediate range order is also important to understand the dynamics: In NS2 the sodium ions that move through channels in the Si–O matrix and the structure of these channels is connected with the prepeak in the static structure factor at 0.95 Å^{-1}. The presence of these channels leads to a surprising decoupling of the fast (single particle) sodium motion from correlations between different sodium atoms that decay on the time scale of the channel relaxation.

Acknowledgments: We thank the HLRZ Stuttgart for a generous grant of computer time on the CRAY T3E. A. W. is grateful to SCHOTT Glas for partial financial support.

References

1. C. A. Angell, J. H. R. Clarke, and L. V. Woodcock, Adv. Chem. Phys. **48**, 397 (1981).
2. U. Balucani and M. Zoppi, *Dynamics of the Liquid State* (Clarendon Press, Oxford, 1994).
3. W. Kob, J. Phys.: Condens. Matter **11**, R85 (1999).
4. P. H. Poole, P. F. McMillan, and G. H. Wolf Reviews in Mineralogy **32**, 563 (1995).
5. K. Vollmayr, W. Kob, K. Binder, Phys. Rev. B **54**, 15808 (1996).
6. J. Horbach, W. Kob, and K. Binder, J. Phys. Chem. B **103**, 4104 (1999).
7. J. Horbach and W. Kob, Phys. Rev. B **60**, 3169 (1999).
8. J. Horbach and W. Kob, Phys. Rev. E **64**, 041503 (2001).
9. J. Horbach, W. Kob, and K. Binder, p. 186 in *High Performance Computing in Science and Engineering '98*, Eds.: E. Krause and W. Jäger (Springer, Berlin, 1999).
10. K. Binder, J. Non–Cryst. Sol. **274**, 332 (2000).
11. P. Scheidler, W. Kob, A. Latz, J. Horbach, and K. Binder, Phys. Rev. B **63**, 104204 (2001).
12. J. Horbach, W. Kob, and K. Binder, Eur. Phys. J. B **19**, 531-543 (2001).
13. A. Roder, W. Kob, K. Binder, J. Chem. Phys. **114**, 7602 (2001).
14. C. Mischler, W. Kob, and K. Binder, Comp. Phys. Comm. (in press).
15. J. Horbach, C. Mischler, W. Kob, and K. Binder, *Multiscale Computer Simulations in Physics, Chemistry, and Biology: The Example of Silica*, Invited paper at the NATO ARW, Kiev, Ukraine, September 9–12, 2001, "Frontiers in Molecular–Scale Science and Technology of Nanocarbon, NanoSilicon and Biopolymer Multifunctional Nanosystems" (E. Buzaneva, P. Scharff, eds.), Kluwer Academic Press, Dordrecht, 2002, p. 1–15.
16. J. Horbach and W. Kob, Phil. Mag. B **79**, 1981 (1999)
17. J. Horbach, W. Kob, and K. Binder, Chem. Geol. **174**, 87 (2001).
18. J. Horbach, W. Kob, and K. Binder, Phys. Rev. Lett. **88**, 125502 (2002).
19. P. Jund, W. Kob, and R. Jullien, Phys. Rev. B **64**, 134303 (2001).
20. R. D. Banhatti and A. Heuer, Phys. Chem. Chem. Phys. **3**, 5104 (2001).
21. N. Zotov, I. Ebbsjo, D. Timpel, and H. Keppler, Phys. Rev. B **60**, 6383 (1999).
22. J. Oviedo and J. F. Sanz, Phys. Rev. B **58**, 9047 (1998).
23. A. Winkler, Ph. D. Thesis (Mainz University, 2002).
24. G. J. Kramer, A. J. M. de Man, and R. A. van Santen, J. Am. Chem. Soc. **64**, 6435 (1991).
25. B. W. van Beest, G. J. Kramer, and R. A. van Santen, Phys. Rev. Lett. **64** 1955 (1990).
26. S. Ispas, M. Benoit, P. Jund, and R. Jullien, Phys. Rev. B **64**, 214206 (2001).
27. D. Frenkel and B. Smit, *Understanding Molecular Simulation — From Algorithms to Applications* (Academic Press, San Diego, 1996).
28. V. F. Sears, J. Mater. Res. **3**, 29 (1992).
29. A. Meyer, H. Schober, and D. B. Dingwell, Europhys. Lett. (in press).